ISSN 2314-5609
Nuclear Sciences Scientific Journal
12, 25-49
2023
https://nssi.journals.ekb.eg

Nuclear Materials Authority
P.O.Box 530 Maadi, Cairo, Egypt

MINERALOGY, GEOCHEMISTRY AND RADIOACTIVITY OF GRANITIC ROCKS AND ASSOCIATED FLUORITE-QUARTZ VEINS, GABAL ADEDIA, UM BOGMA AREA, SOUTHWESTERN SINAI, EGYPT

DOAA A. MOSTAFA
Nuclear Materials Authority, P. O. Box 530, El-Maadi, Cairo, Egypt

ABSTRACT

Mineralogical, geochemical and radioactive studies were carried out on both the granitic rocks of Gabal Adedia and its associated quartz-fluorite veins. The radioactive fluorite veins are filling the fissures and fractures of the host granite at the base of Gabal Adedia, the fluorite present in two forms as coarse-grained crystals disseminated in the younger granite or associated with quartz veins.

The mineralogical investigations of the younger granite and its associated quartz-fluorite veins revealed the presence of secondary uranium mineral (kasolite), in addition to uranothorite, Fergusonite, monazite, allanite, bastnaesite, fluorite, zircon, xenotime, apatite, pyrite, barite, galena, chalcopyrite, sphalerite, covellite, bornite and atacamite.

The studied granite and associated quartz-fluorite veins show enrichment in some rare metals (Cu,Zn,Zr,Y,Ba,Pb,Nb,U and Th) mineralizations. Multistage deformation, magmatic and hydrothermal processes accompanied by the events of uranium mineralization with the associated rare metals mineralization in different episodes affected Gabal Adedia. The normalized REE pattern of the younger granite and associated fluorite-quartz veins display negative Eu anomaly (Eu/Eu*= 0.54, 0.76) respectively. The younger granite is characterized by enrichment of LREE, in contrary the fluorite-quartz veins are enriched in HREE. Allanite, bastnaesite and monazite which are the most important REE carriers in this granite. These minerals are strongly enriched in LREE, whereas fluorite and xenotime which are more abundant in fluorite-quartz veins are enriched in HREE. The negative cerium (Ce) anomolia indicate high oxygen (O) fugacity at the source of the hydrothermal fluids. Positive yttrium (Y) anomalia articulate strong complexation with fluorite (F).

The studied rocks have slightly high uranium and thorium contents, the younger granite have average U content is 27 ppm and the average of Th content is 54.4 ppm while in fluorite-quartz veins the average U content is 152.4 ppm and the average of Th content is 57.8 ppm.

INTRODUCTION

The studied area is located at southern Sinai Peninsula 40 km east of Abu Zeneima city. Gabal Adedia is characterized by high to moderate relief terrain, which is covered with high topographic Paleozoic sedimentary rocks (Fig. 1)

Bishr (2003) studied the fluorite-bearing quartz veins that present in the younger granite of G. Adedia and stated that the radiometry

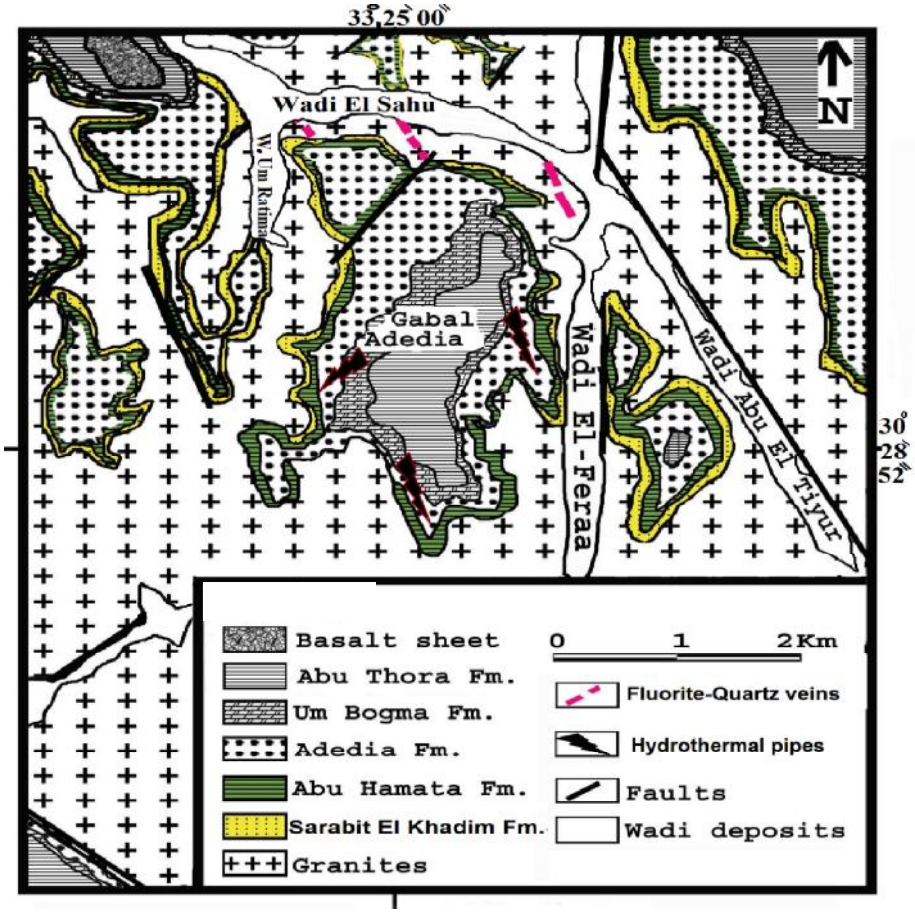

Fig. 1: Geologic map of the studied area (Bishr and Nasr 2017)

measurements along these veins are high due to the presence of secondary uranium mineral kasolite.

Ali (2016) concluded that younger granite of Adedia is subalkaline and peraluminous originated in extensional regime belonging to I-type granite and developed in post-collision granite environment.

According to Bishr and Nasr (2017), two hydrothermal events can be expected in the area; the first took place during the Late Precambrian terminated with the granite rocks represented by the fluorite-quartz veins. The second Phanerozoic hydrothermal event which related to the Early Carboniferous terminated with upper Um Bogma Formation through the hydrothermal pipes.

Fluorite is widely distributed among the basement rocks of Egypt. It is formed during a late magmatic crystallization of the younger granite as dissemination or as late-crystallization hydrothermal deposits (Sabet et al., 1976 and Hussein, 1990).

Fluorite (CaF_2), commercially known as fluorspar, is an important mineral that is used as a raw material in the metallurgy, ceramics and chemical industries apart from optical and lapidary uses (Magotra et al., 2017). Fluorite may be deposited together with rare earth element (REE) - bearing minerals, in mining areas associated with pegmatitic and hydrothermal stages, in weathering and sedimentary environments within sedimentary, metamorphic and igneous rocks (Chakhmouradian et al., 2012). Therefore, REE Patterns and trace elements could reflect the source from which they crystallized or precipitated (Sallet et al., 2000).

The present study deals with the field, mineralogy, geochemistry and radioactivity of the younger granite and associated fluorite-quartz veins in the area of Gabal Adedia.

GEOLOGIC SETTING

The area under consideration is occupied by high and sharp igneous elevations of the Arabian Nubian Shield covered with Paleozoic rocks. The granitic rocks at the studied area South Wadi El Sahu are nonconformably overlain by thick sequence of Phanerozoic sedimentary rocks of Sarabit El Khadim, Abu Hamata, Adedia, Um Bogma and Abu Thora formations (Fig. 2). The extremely radioactive spots are related to the fractured areas at the base of Gabal Adedia, which are characterized by the presence of parallel NE-SW trending fluorite-bearing quartz veins (Fig. 3), rich with visible uranium minerals. The highly radioactive fluorite-bearing quartz veins in the studied granite appear in violet colors and associated with green copper staining.

The granite rocks are the most dominant rocks exposed in the area, which are referred to Gattarian granites (Hume, (1935), younger granites (El-Ramly and Akaad, 1960), late-to post-orogenic granites (El-Gaby, 1975).

The studied younger granite is medium-to coarse-grained with pinkish white color and composed of K-feldspar, plagioclase and quartz surrounded with fine-grained groundmass of the similar components. They show strong columnar jointing and fracturing pattern with well-developed six sided faces (Fig. 4); such joints are due to shrinkage during magma solidification.

The younger granite of the studied area represent high rugged terrains. They form very high relief mountains and show moderate to high degree of weathering. The cavernous

Fig.2 : Photograph showing the southern part of Gabal Adedia, (Wadi El-Feraa)

Fig.3: Photograph showing Fluorite-rich quartz-radioactive veins in the granite rock

Fig.5: Photograph showing monumental shape and exfoliation in the granites

Fig.4: Photograph showing well developed columnar jointing and fracturing of granites

weathering, exfoliation and monumental shapes (Fig. 5) may be present. The area is mainly dissected by normal faults striking N-S, NNW-SSE and NW-SE as well as strike-slip faults of NW-SE and NE-SW trends.

Fluorite is present in two forms as coarse-grained crystals disseminations in the younger granites and can be seen by naked eyes. Also, fluorite present associated with quartz veins. The radioactive veins described as fluoritization zone and distinguished by greenish color of copper and uranium mineralization, which seen by the naked eyes in the field. The veins range in thickness from few centimeters up to 25 centimeters and reaching up to 10 meters in length in granite rocks. They exhibit intrusive sharp contacts with the surrounding granite of Gabal Adedia.

The field observation showed that the studied area affected by hydrothermal solutions reflected in different alteration phases as hematitization and kaolinitization (Fig. 6).

PETROGRAPHIC CHARACTERISTICS

Megascopically, the studied granite (monzogranite) is characterized by grayish pink color and medium-to coarse grains with equigranular crystals. It is essentially composed of plagioclase, alkali feldspar and quartz associated with mafic minerals represented by biotite and muscovite.

Plagioclase represents about 37.4% of the forming minerals. It occurrs as subhedral to euhedral crystals of oligoclase (An26) exhibiting its characteristic lamellar twinning. Some crystals are characterized by normal zoning. Most of the plagioclase crystals are saussuritized (Fig. 7) by post-magmatic processes. Alkali feldspars are present as string perthite crystals and as orthoclase perthite crystals enclosing finer crystals of plagioclase (Fig. 8). Quartz represents about 28.5% of the rock. It occurs as anhedral to subhedral crystals filling the interstitial spaces between the other constituents and associating the feldspars. Mafic minerals are represented

Fig.6: Photograph showing hematitization and kaolinitization along fractures in the granites

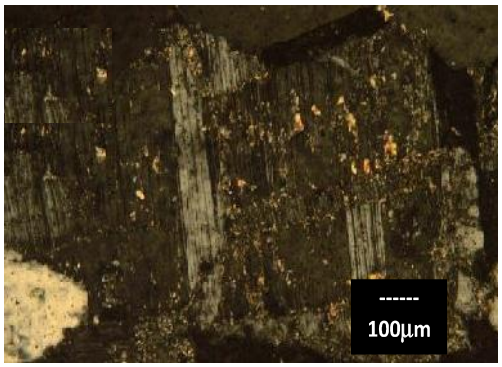

Fig.7: Subhedral crystal of plagioclase showing saussuritization and muscovitation

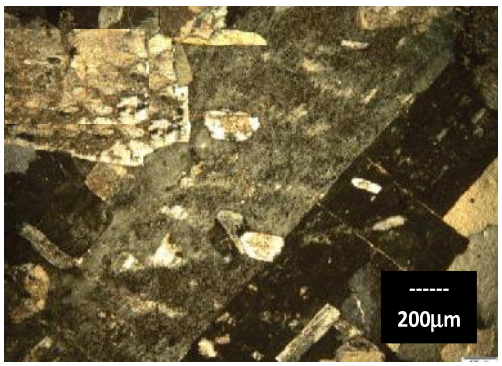

Fig.8: Orthoclase perthite crystal enclosing fine crystal of plagioclase

by biotite and muscovite and occupy about 2.6% of the rock. Biotite is the main mica occurring as anhedral flakes with strong pleochroism from brown to dark brown; some crystals are considered as good host for most of the accessory minerals (Fig. 9). Primary muscovite is also present as flakes exhibiting its characteristic high interference colours.

Accessory minerals are mainly zircon, fluorite, uranium and thorium minerals. Zircon is the most abundant accessory mineral. It occurs as zoned euhedral crystals, it is included in quartz (Fig. 10). Fluorite is found as large crystals of colorless and violet colors exhibits subhedral interstitial crystals. Cubic crystal of uranothorite surrounded by nucleoid haloes (Fig. 11), these haloes result from the radiation effects of the included radio elements.

The veins are essentially composed of fluorite, quartz and calcite. The fluorite is found as veinlets of colorless to violet colors (Fig. 12). Along the fractures, copper staining are abundant. Calcite is present as anhedral crystals associated with quartz and sericite (Fig. 13). The feldspars are altered to sericite (Fig.14), sericitization to feldspars is due to thermal effects when the fluorite veins intruded the granite.

MINERAL COMPOSITION

The heavy minerals were separated from the monzogranite and associated fluorite-quartz veins by heavy liquid and picked as individual minerals under the binocular microscope. These minerals were identified by Environmental Scanning Electron Microscope (ESEM) using back-scattered imaging, EDAX analyses and confirmed by X-ray diffraction (XRD) techniques.

The studied mineralization of granitic rocks and fluorite-quartz veins of Adedia area can be classified into the following groups: 1) U-Th-REE-bearing Minerals, 2) Accessory Minerals, 3) Sulphides and chlorides minerals.

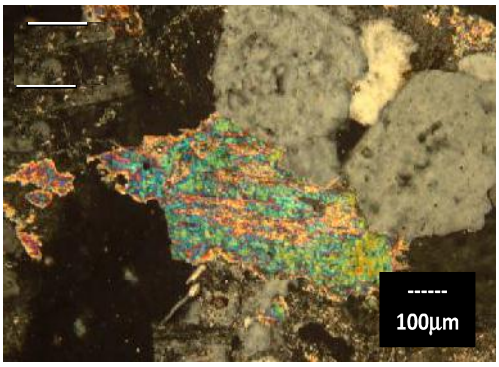

Fig. 9: Muscovitized biotite associating quartz and plagioclase

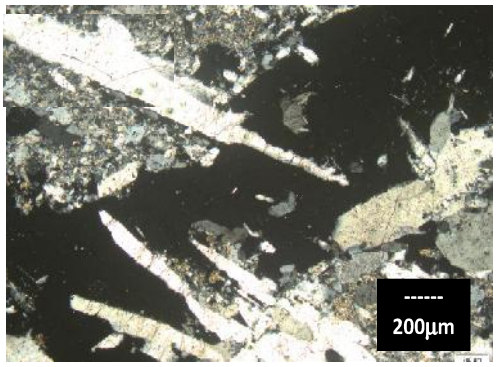

Fig. 12: Veinlet of fluorite associated with quartz

Fig.10: Photograph showing euhedral crystal of zircon included in quartz

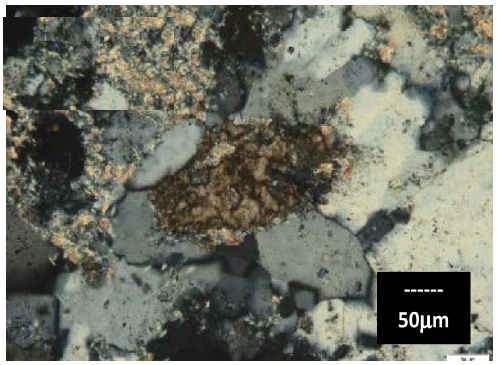

Fig.13:Calcite crystal associating quartz and sericit

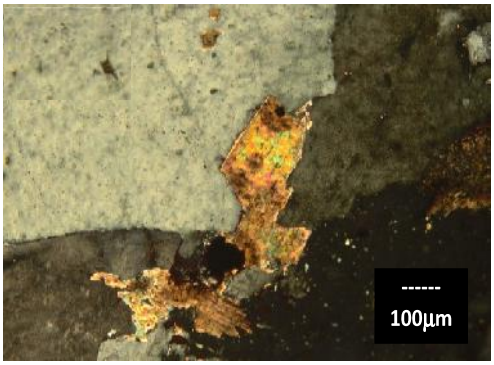

Fig.11:Nucloid haloes surrounded uranothorite crystal

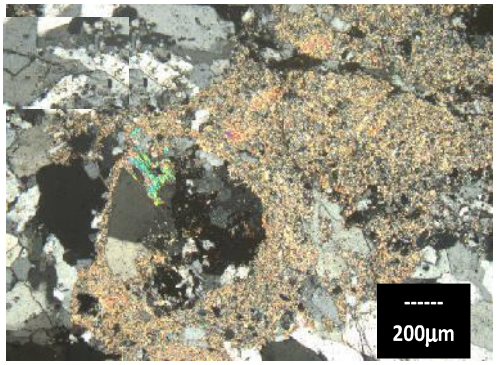

Fig. 14: Feldspars altered to sericite

U-Th-REE-bearing Minerals

Kasolite ($Pb(UO_2)\ SiO_4.H_2O$) is common secondary uranium mineral recorded in the fluorite-quartz veins associated with copper minerals. Kasolite occurs as massive granular masses having resinous to greasy luster and yellow color (Fig. 15). Kasolite is identified by X-ray diffraction analysis associated with fluorite mineral (Fig. 16) and the EDX semi-quantitative analysis indicates that the studied kasolite has 50.99% U, 39.72% Pb and 9.29% Si (Fig.17).

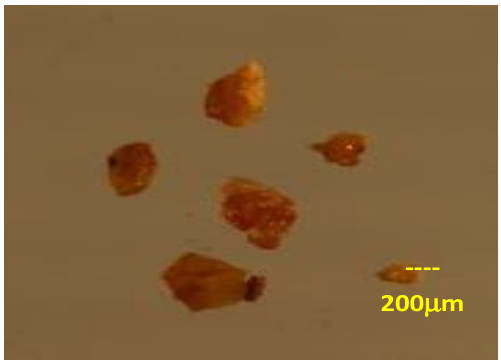

Fig.15: Photograph showing kasolite

Uranothorite ($Th,U,Ce)SiO_4$ is a uranium-rich variety of thorite, containing up to half of thorium replaced by uranium. It occurs as minute crystals in the studied granite. Uranothorite have crystals with yellowish brown to brown color (Fig. 18) with vitreous and resinous luster. ESEM and semi-quantitative EDAX analyses, (Fig. 19), show that the uranothorite has U content 17.63% and Th reaching up to 42.79%.

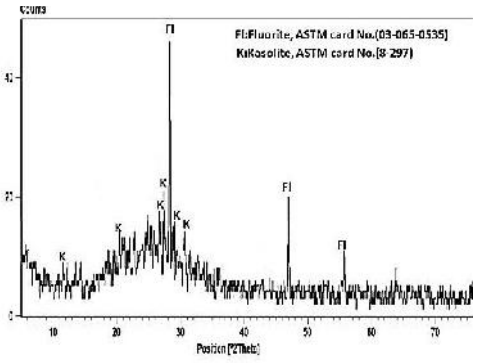

Fig.16: X-ray diffraction pattern of kasolite associated with fluorite

Fergusonite [(Y,Er) $(Nb,Ta,Ti)O_4$] is an accessory mineral containing significant quantities of U and Th, and is commonly metamict (Reto et al., 2009). The X-ray diffraction recorded fergusonite mineral associated with galena (Fig. 20).

Monazite [$(Ce,La,Th,Nd,Y)PO_4$] is a chief rare earth-bearing phosphate mineral occurring as accessory mineral in the studied granitic rocks. Th-poor monazite might be used to fingerprint its potential sources which comprise allanite as well as leaching or replacement of fluorapatite (Pan and Breaks, 1997). From the EDX data (Fig. 21), monazite contains an average 19.94% Ce, 9.92% La, 10.25% Nd, 4.18% Sm, 3.63% Pr, 4.25% Gd 2.01% Th, and 14.87% P.

Allanite [$(Ce,Ca,Y,La)\ (Al,Fe^{+3})_3(SiO_4)_3$. OH] varies in color from light brown to black (Fig.-22). Due to its similarity to the rare earth elements in ionic radius, U and Th may be

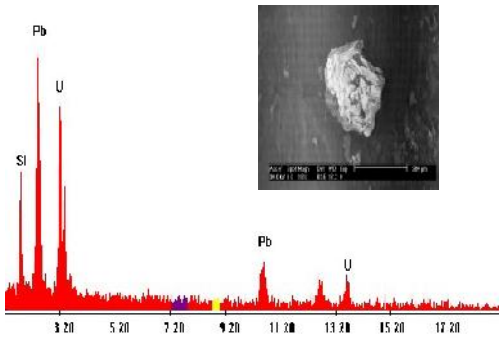

Fig. 17: ESEM image and EDX analysis data of kasolite

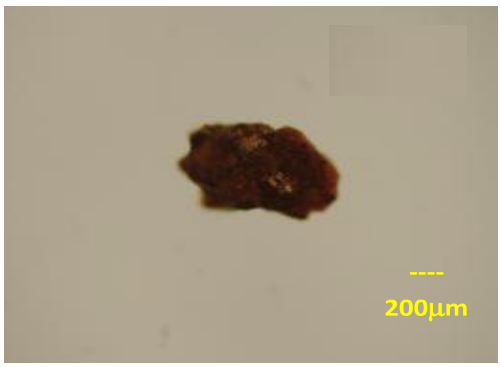

Fig. 18: Photograph showing uranothorite

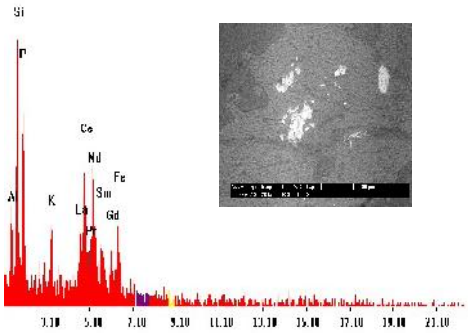

Fig.21: ESEM image and EDX analysis data of monazite

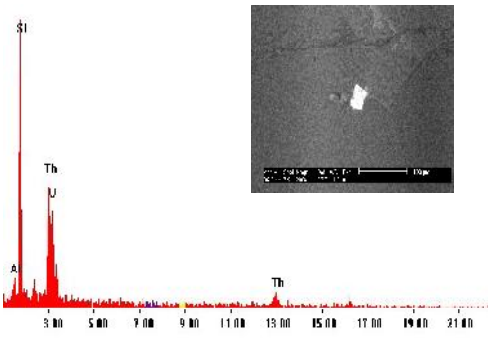

Fig. 19: ESEM image and EDX analysis data of Uranothorite

incorporated in the structure of allanite. EDX data show that allanite is composed essentially of LREE, Fe, Ca, Al and Si as well as U and Th content (Fig. 23).

Bastnaesite [(Ce,La,Nd)(CO_3)F] is one of the world's primary sources for REE's and is dominated by LREE's (Hedrick, 2004). Bastnaesite is transparent to translucent ranges in color from wax-yellow to reddish-brown with vitreous luster. It was confirmed by ESEM technique (Fig. 24).

Zircon ($ZrSiO_4$) is a remarkable mineral due to its ubiquitous occurrence in crustal igneous, sedimentary and metamorphic rocks,

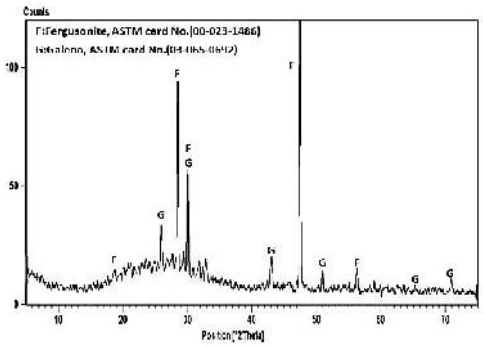

Fig. 20: X-ray diffraction pattern of fergusonite associated with galena

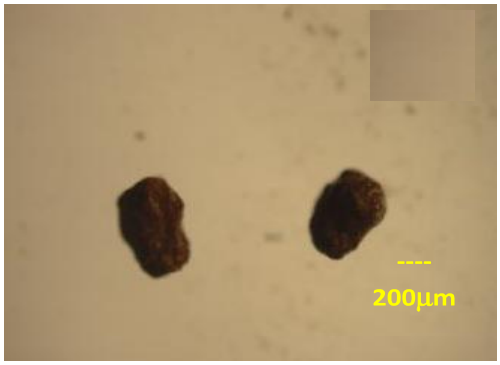

Fig.22: Photograph showing allanite

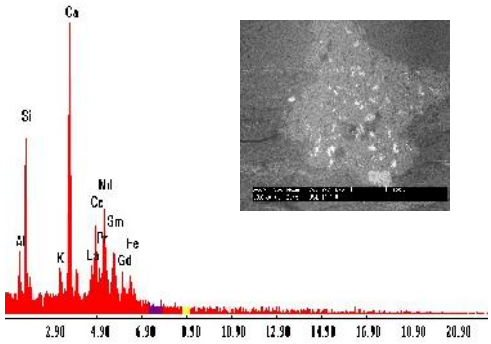

Fig. 23: ESEM image and EDX analysis data of Allanite

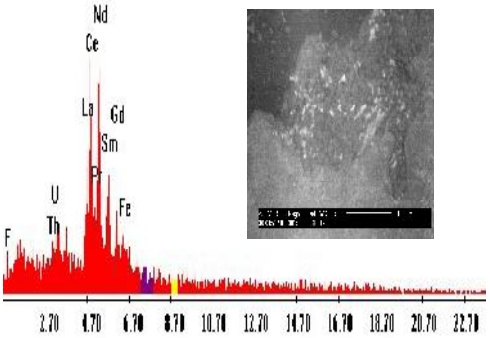

Fig. 24: ESEM image and EDX analysis data of Bastnaesite

and in even mantle xenoliths, lunar rocks, meteorites and tektite (Speer, 1980). Read (1984) suggested that uranium is the most important trace element in zircon. Zircon is characterized by its bi-pyramidal prismatic crystals as recorded in the granite of G. Adedia (Fig. 25). The X-ray diffraction analysis detected the presence of zircon mineral (Fig. 26). EDX semi-quantitative analysis of zircon mineral (Fig. 27). The existence of Y, P, Th, U and REE may assign to the association of xenotime and uranothorite as solid solution with zircon (Fig. 28).

Xenotime (YPO_4) is a rare earth phosphate mineral, whose major component is yttrium orthophosphate. Xenotime occurs as massive form, ranging in color from pale yellow to yellowish pale brown with greasy luster (Fig. ~~4e~~ 29). The EDX analyses gave, P (20.58%) Y (37.16%) Yb (5.46%) Er (3.66%) and Fe (7.87%) (Fig. 30).

Accessory Minerals

Fluorite (CaF_2) presents in veins and is the most common mineral in the study area. Fluorite of the studied area exhibit wide range of colors from colorless (Fig. 31), pale blue to dark violet (Fig. 32) with vitreous

Fig.25: Photograph showing zircon

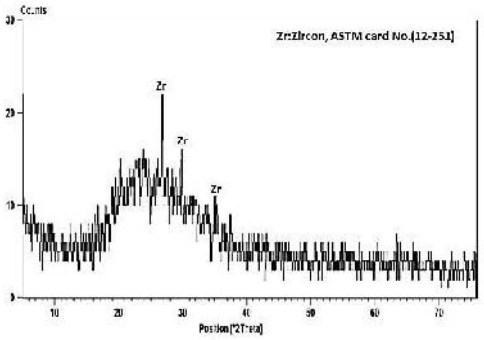

Fig.26: X-ray diffraction pattern of zircon

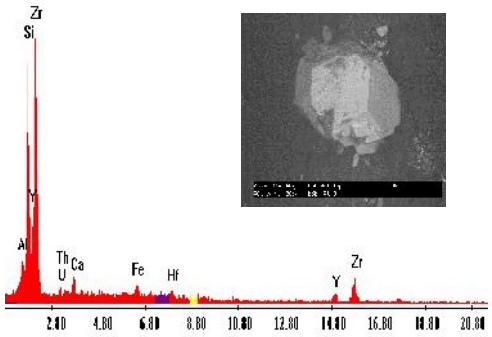

Fig.27 : ESEM image and EDX analysis data of Zircon

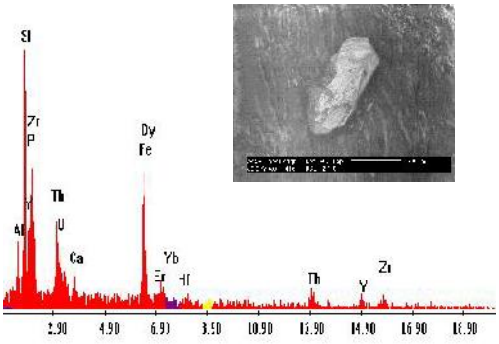

Fig.28 : ESEM image and EDX analysis data of Zircon

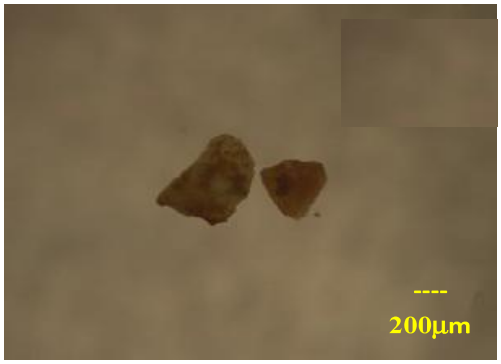

Fig. 29 : Photograph showing xenotime

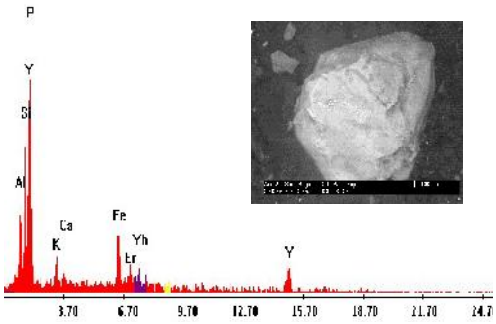

Fig.30: ESEM image and EDX analysis data of Xenotime

and resinous luster. In the present study it is chiefly observed as veins in the granitic rocks. The presence of violet fluorite suggests the epigenetic hydrothermal origin associated with the uranium mineralization (Salman et al., 1986, Roz., 1994 and Shalaby, 1995). It is identified by X-ray diffraction analysis associating quartz (Fig. 33). The EDX analysis (Fig. 34) shows that Fluorite contains an average 66.42% Ca and 26.46% F.

Apatite ($CaPO_4$) occurs as rounded to subrounded crystals of white to yellow color (Fig. 35) with vitreous to greasy luster. The X-ray diffraction analysis recorded fluorapatite mineral (Figs. 36). The EDX semi-quantitative analysis and ESEM image gave 3.56% Ca and 20.29% P % (Fig. 37).

Barite ($BaSO_4$) is the main ore of barium, occurs chiefly in medium-to low temperature hydrothermal vein deposits as gangue mineral (Berry et al., 2000). Barite crystals occur as reddish brown to pale brown transparent to translucent and have vitreous luster. Barite was confirmed by ESEM technique (Fig.-38).

Sulphides and chlorides minerals

Sulphides and chlorides are relatively common in the studied rocks. They are represented by pyrite (FeS_2), galena (PbS_2), chalcopyrite ($CuFeS_2$), covellite (CuS), bornite (Cu_5FeS_4)

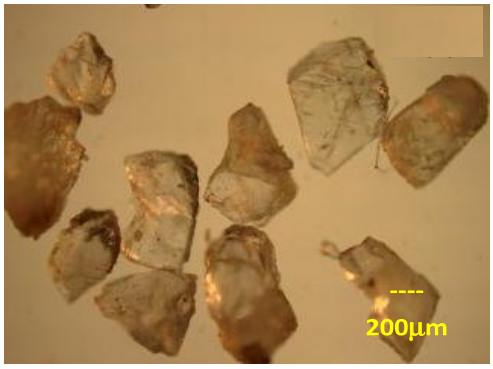

Fig.31: Photograph showing colorless fluorite

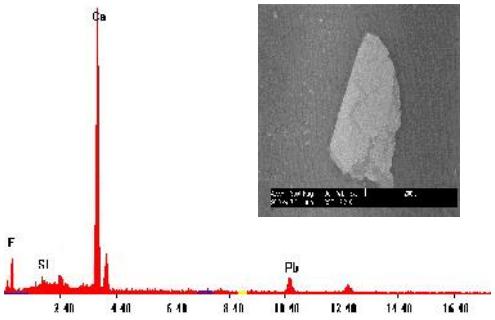

Fig. 34: ESEM image and EDX analysis data of Fluorite

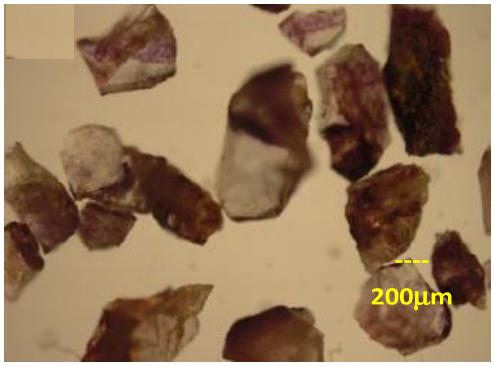

Fig. 32: Photograph showing violet fluorite

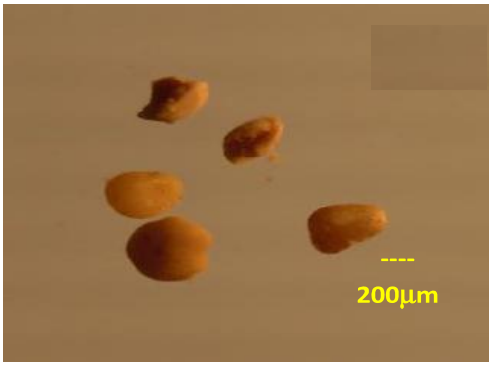

Fig.35: Photograph showing apatite

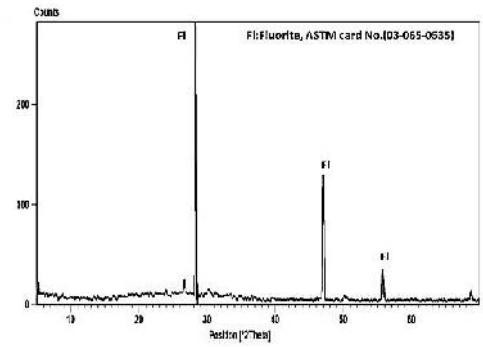

Fig.33: X-ray diffraction pattern of fluorite

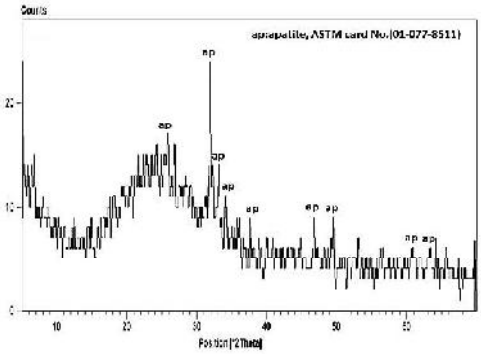

Fig. 36: X-ray diffraction pattern of apatite

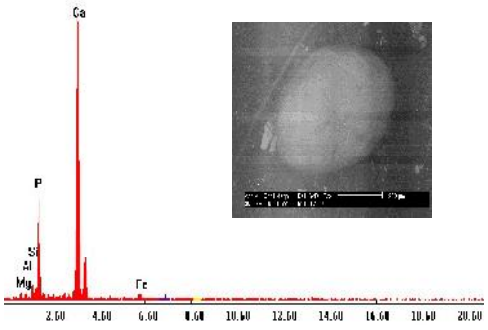

Fig. 37: ESEM image and EDX analysis data of Apatite

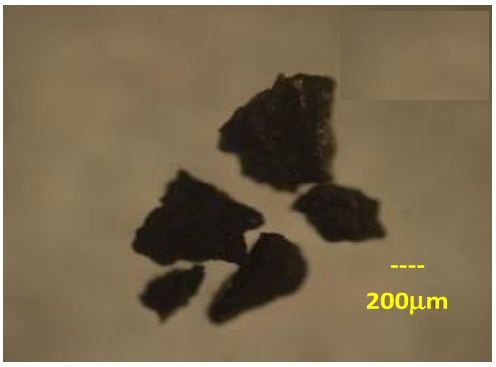

Fig.39: Photograph showing flakes of galena

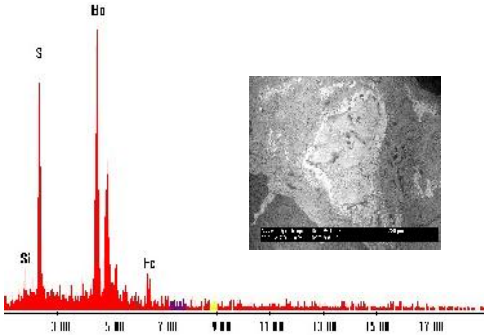

Fig.38: ESEM image and EDX analysis data of Barite

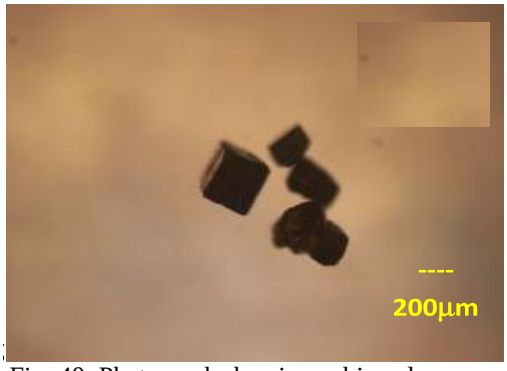

Fig. 40: Photograph showing cubic galena

and Atacamite [$Cu_2Cl(OH)_3$].

Galena (PbS) is a primary minerals, it is the most common mineral containing lead. Galena occurs most frequently together with sphalerite. Occurrence of lead and zinc sulphide may be of low-, intermediate- or high temperature origin (Deer et al., 1992). Galena was found in two shapes as flakes (Fig. 39)or as cubic-octahedral crystals (Fig. 40). Galena is identified by X-ray diffraction associated with fergusonite mineral (Fig. 41) and EDX semi-quantitative analysis data shows that galena has 73.71% Pb and 9.19% S (Fig. 42).

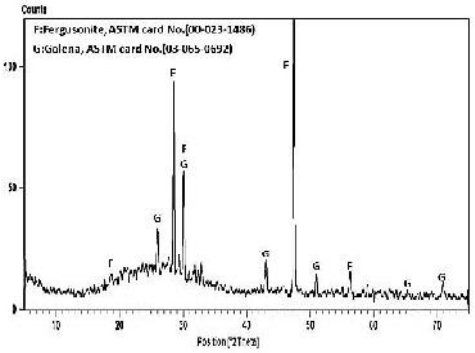

Fig. 41: X-ray diffraction pattern of fergusonite associated with galena

Sphalerite (Zn,Fe)S occurs as well-formed crystals of olive-green and yellow colors (Fig. 43). It is transparent with greasy luster and brownish white streak. It is identified by X-ray diffraction analysis associated with galena mineral (Fig. 44). EDX semi-quantitative analysis data shows that sphalerite have 54.30% Zn, 35.44% S, 8.20% Cu and 2.06 Fe (Fig. 45).

Pyrite (FeS_2) is by far the most widespread and commonly occurring sulfide mineral. It can be found in almost any type of geologic environment (Berry et al., 1983). Pyrite has pale-brass yellow color and metallic luster (Fig. 46). X- ray diffraction analysis is recorded the presence of pyrite mineral (Fig. 47) and EDX analysis data show that pyrite composed of 44.21% Fe and 55.79% S (Fig. 48).

Chalcopyrite ($CuFeS_2$) is the most important copper ore. It crystallizes in the tetragonal system and occurs in ore veins deposited at medium and high temperatures. It has a brassy to golden yellow color (Fig. 49). The X-ray diffraction analysis detected the presence of chalcopyrite (Fig. 50). EDX semi-quantitative analysis data shows that chalcopyrite has 38.71% Cu, 27.82% Fe and 30.76% S (Fig. 51).

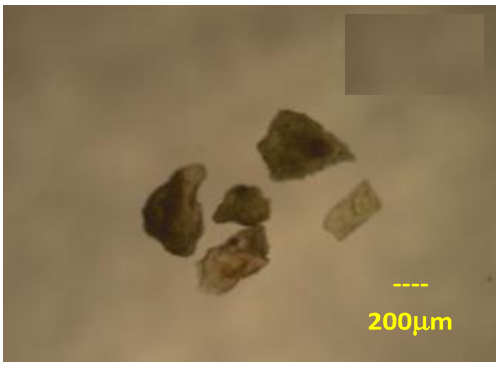

Fig. 43: Photograph showing sphalerite

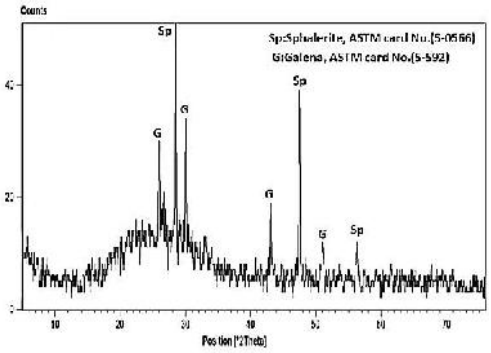

Fig. 44: X-ray diffraction pattern of sphalerite

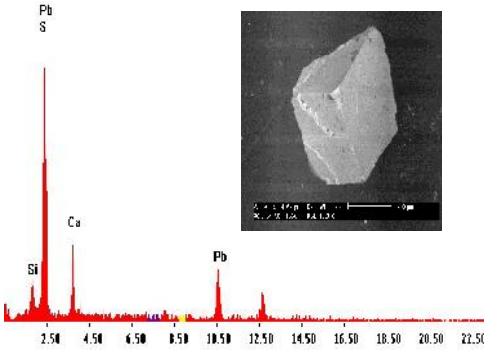

Fig. 42: ESEM image and EDX analysis data of Galena

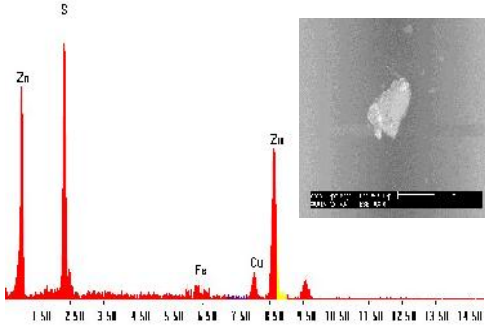

Fig. 45: ESEM image and EDX analysis data of Sphalerite

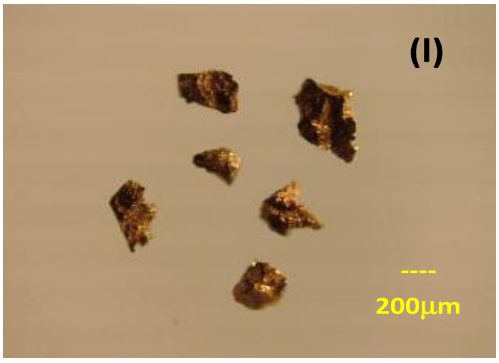

Fig.46: Photograph showing pyrite

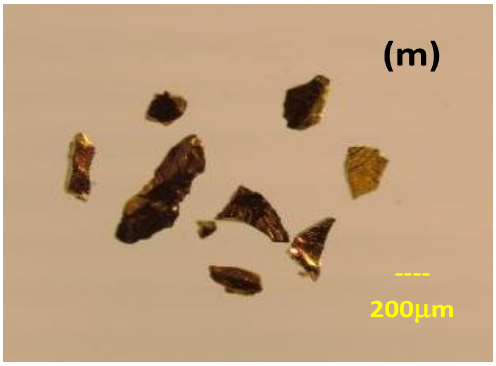

Fig.49: Photograph showing chalcopyrite

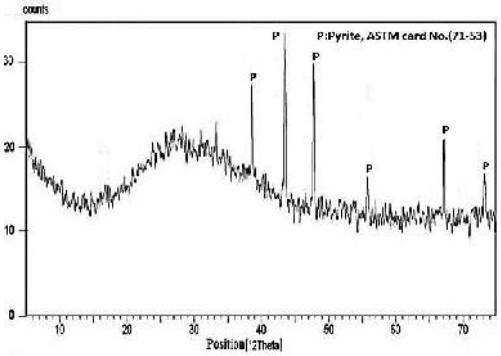

Fig. 47: X-ray diffraction pattern of pyrite

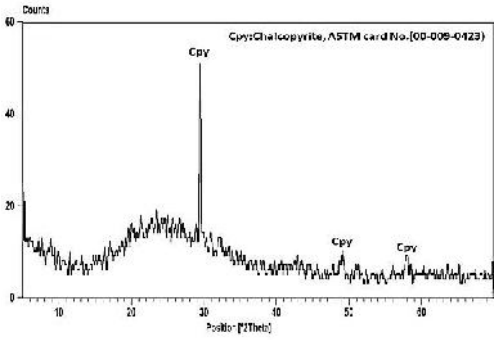

Fig.50: X-ray diffraction pattern of chalcopyrite

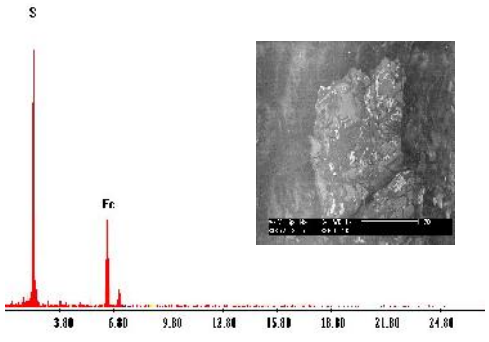

Fig. 48: ESEM image and EDX analysis data of Pyrite

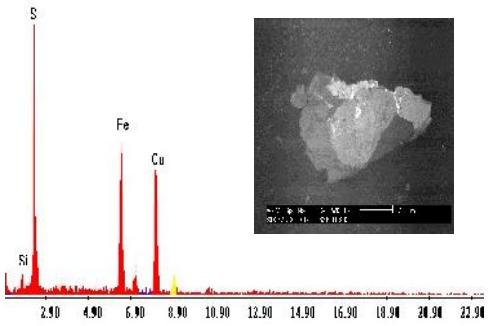

Fig. 51: ESEM image and EDX analysis data of Chalcopyrite

Covellite (CuS) is a rare copper sulphides found in zones of secondary enrichment (supergene) of copper sulphide deposits and found as coatings on sulphide minerals. Covellite has indigo blue color (Fig.52) with resinous to dull luster. It is identified by X-ray diffraction associated with quartz and calcite (Fig.53). EDX semi-quantitative analysis data shows that covellite have 76.16% Cu and 12.11% S (Fig. 54).

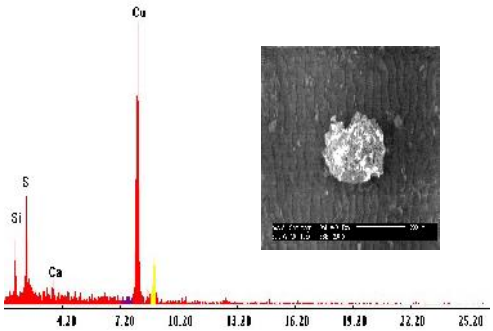

Fig. 54: ESEM image and EDX analysis data of Covellite

Bornite (Cu_5FeS_4) forms as a primary hydrothermal precipitate or a later supergene replacement mineral. It occurs with other copper minerals such as covellite and chalcopyrite. It is marked by its intense purple to blue iridescence (Fig.-55). The X-ray diffraction analysis recorded bornite associated with galena, quartz and fluorite minerals (Fig. 56). EDX semi-quantitative analysis data shows that bornite have 50.22% Cu, 12.14% Fe and 26.70% S (Fig.- 57).

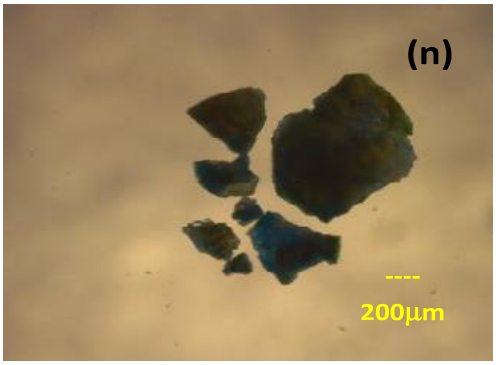

Fig.52: Photograph showing covellite

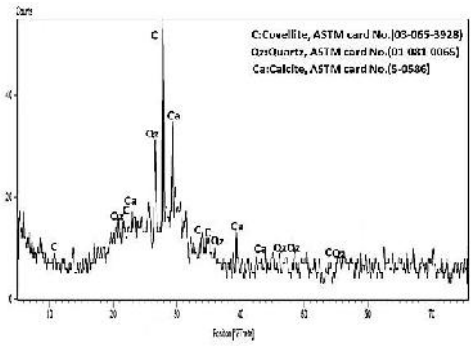

Fig. 53: X-ray diffraction pattern of covellite associated with quartz and calcite

Atacamite [$Cu_2Cl(OH)_3$] is a secondary copper mineral formed from primary copper minerals in the oxidation or weathering zone. Atacamite is massive and characterized by green color (Fig.58). The EDX analysis revealed that atacamite contains 75.33% Cu and 20.65% Cl (Fig. 59).

GEOCHEMISTRY

Analytical Methods

Ten samples were collected from the investigated granite (five samples from the monzogranite and five samples from its associated fluorite-quartz veins). They were analyzed for trace and REEs at the Egyptian nucleur materials authority labs (NMA). Trace elements are determined by X-ray fluorescence technique (XRF) using PHILIPS X'Unique-II spectrometer with automatic sample changer PW 1510. REEs measured using ICP-AES, Perkin Elmer and optima 3000 instrument. The accuracy of the results was found to be in the range 5-10% for the trace and rare earth

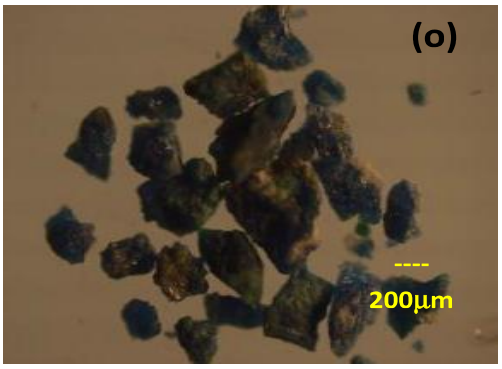

Fig.55: Photograph showing bornite associated with galena

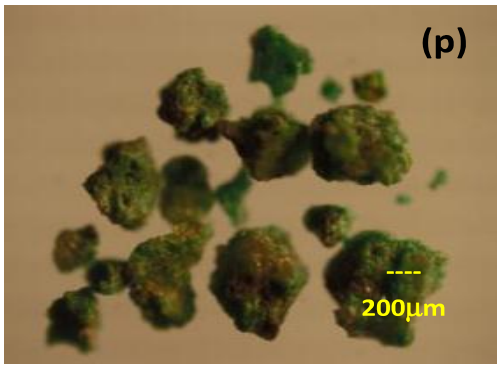

Fig.58: Photograph showing atacmite

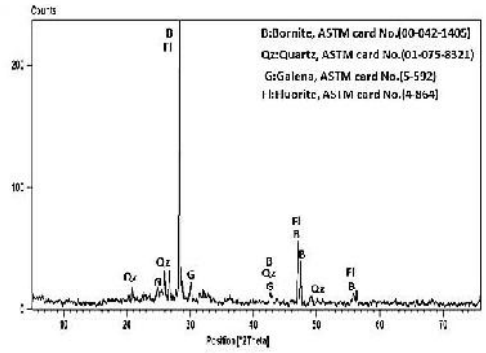

Fig. 56: X-ray diffraction pattern of bornite associated with quartz, fluorite and galena

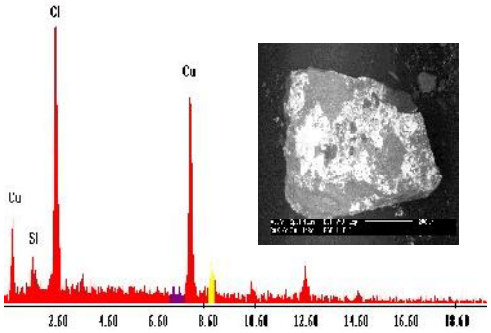

Fig. 59: ESEM image and EDX analysis data of Atacmite

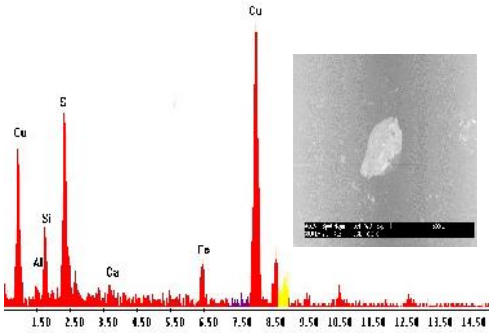

Fig. 57: ESEM image and EDX analysis data of Bornite

elements. The results of these analyses are listed in Table (1).

Geochemistry of Trace Elements

The presence of enrichment-depletion trends for minor elements is due to the variation of the physio-chemical conditions of the fluids, such as the Ph, Eh, temperature, and ionic complexes during the development of the deposit (Karakaya et al., 2011). Concentrations of a wide variety of trace elements in Table (1) shows that the enrichment in some rare metal contents (Cu,Zn,Zr,Y,Ba,Pb,Nb,U and Th) reaching up to average (57.8, 232,

Table 1 : U, Th, trace and REEs analyses of monzogranite and fluorite-quartz veins, G. Adedia.

Rock	Monzogranits						Fluorite-quartz veins					
Samples	Ad5	Ad6	Ad7	Ad8	Ad9	aver	Ad1	Ad2	Ad3	Ad11	Ad12	aver
Radioelements(ppm)												
U	28	16	30	32	29	27	107	213	280	83	79	152.4
Th	72	48	50	46	56	54.4	83	50	67	49	40	57.8
Th/U	2.57	3.00	1.67	1.44	1.93	2.01	0.78	0.23	0.24	0.59	0.51	0.38
Trace elements(ppm)												
Cr	237	152	300	160	147	199.2	184	159	153	245	95	167.20
Ni	8	7	9	6	7	7.4	8	9	6	8	6	7.40
Cu	138	16	114	10	11	57.8	388	203	193	94	11	177.80
Zn	601	401	91	38	29	232	443	232	378	46	71	234.00
Zr	137	166	59	140	151	130.6	148	155	132	83	55	114.60
Rb	206	424	173	504	561	373.6	180	270	141	309	166	213.20
Y	42	168	81	168	197	131.2	250	320	210	185	178	228.60
Ba	101	61	40	103	65	74	156	146	125	38	7	94.40
Pb	354	117	117	20	30	127.6	480	100	582	28	14	240.80
Sr	4	4	2	4	4	3.6	4	4	4	2	3	3.40
Ga	31	21	15	14	5	17.2	2	2	5	2	14	5.00
V	4	3	2	3	2	2.8	4	5	5	2	2	3.60
Nb	26	29	10	26	26	23.4	27	28	25	15	9	20.80
REEs(ppm)												
La	33.25	54.22	42.46	29.34	59.18	43.69	17.2	19.13	12.21	15.54	7.05	14.23
Ce	72.34	89.2	81.39	68.14	103.41	82.90	34.58	37.22	29.57	36.15	23.49	32.20
Pr	9.28	12.67	11.24	7.37	15.07	11.13	4.61	5.04	4.19	5.6	3.71	4.63
Nd	38.39	53.47	48.22	30.28	63.28	46.73	18.85	20.65	14.1	17.54	12.3	16.69
Sm	9.48	13.17	11.09	8.34	15.14	11.44	7.95	8.33	7.35	7.65	6.45	7.55
Eu	1.6	1.88	1.82	1.57	2.02	1.78	0.85	0.94	0.6	0.37	0.25	0.60
Gd	8.31	9.76	9.13	7.48	11.14	9.16	20.01	21.45	16.13	18.55	15.4	18.31
Tb	1.5	2.05	1.88	1.28	2.28	1.80	3.74	4.3	3.15	4.49	2.9	3.72
Dy	12.78	20.37	13.81	11.05	22.8	16.16	33.3	34.2	29.01	36.84	25.46	31.76
Ho	2.03	2.49	2.51	1.64	2.45	2.22	7.97	10.16	6.8	8.2	6.03	7.83
Er	5.92	6.23	6.3	5.61	9.1	6.63	14.7	17.22	13.85	15.52	11.18	14.49
Tm	1.23	1.6	1.72	1.35	2.58	1.70	3.81	4.11	2.6	3.44	2.35	3.26
Yb	24.67	23.12	26.19	16.46	25.15	23.12	11	12.46	8.25	9.4	7.92	9.81
Lu	3.5	2.8	3.67	2.13	3.66	3.15	2.5	5.34	5.05	4.71	3.81	4.28
∑REEs	224.28	293.03	261.43	192.04	337.26	261.61	181.07	200.55	152.86	184	128.3	169.36
∑LREEs	164.34	224.61	196.22	145.04	258.1	197.66	84.04	91.31	68.02	82.85	53.25	75.89
∑HREEs	59.94	68.42	65.21	47	79.16	63.95	97.03	109.24	84.84	101.15	75.05	93.46
Eu/Eu*	0.55	0.51	0.55	0.61	0.47	0.54	0.51	0.52	1.35	0.57	0.83	0.76
Lan/Lun	1	2.03	1.21	1.45	1.70	1.48	0.64	1.01	0.74	0.37	0.28	0.61
Gdn/Lun	0.30	0.44	0.31	0.44	0.38	0.37	0.61	0.71	0.32	0.49	0.32	0.49
Ce/Ce*	1	0.82	0.90	1.12	0.84	0.94	0.97	1.42	1.13	1.34	1.12	1.20
Y/Y*	0.61	1.74	1.01	2.91	1.94	1.64	1.25	1.30	0.8	1.11	0.95	1.08

130.6, 131.2, 74, 127.6 and 23.4 ppm) in monzogranite and (177.8, 234, 114.6, 228.6, 94.4, 240.8 and 20.8 ppm respectively) in fluorite-quartz veins. Figures (60&61) are a 3D histogram illustrates the trace elements values for the monzogranite and fluorite-quartz veins. The high content in some rare metal is due to the hydrothermal fluids lead to the intense alteration. This alteration acts as a trap phase and carrier for some rare metal mineralization. The hydrothermal fluids are potentially important in the dissolution, transportation and precipitation of these elements.

Geochemistry of Rare Earth Elements (REE's)

The REE's are the most useful of all trace elements in the interpretation of the igneous rocks petrogenesis. The REE's are considered to be incompatible with lithophile characters and tend to be concentrated in silicate melts

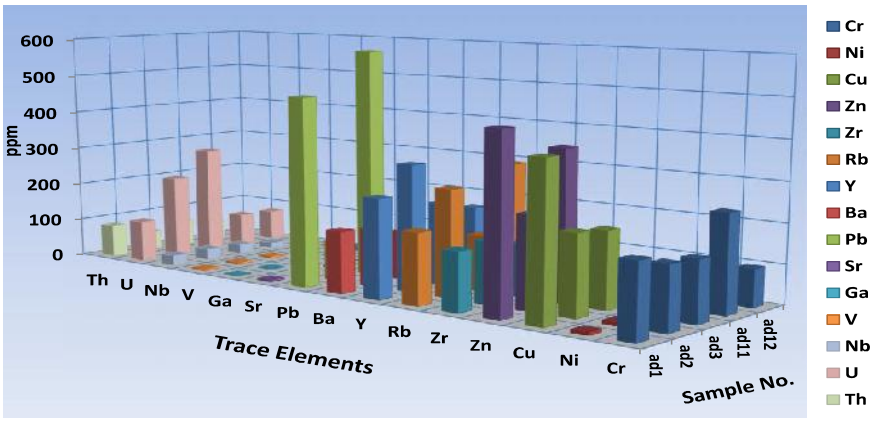

Fig.60: Histogram shows the trace elements content of the monzogranite

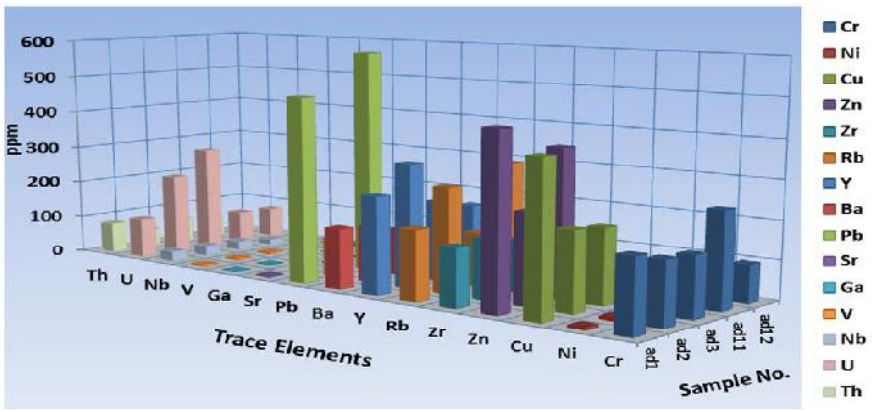

Fig.61: Histogram shows the trace elements content of the

and highly fractionated rocks. Hence The REE's tend to concentrate in the residual magma and occur in the accessory minerals such as allanite, bastnaesite, monazite, zircon, xenotime and fluorite.

According to chondrite values of (McDonough & Sun 1995), the normalized REE pattern of monzogranite and associated fluorite-quartz veins shows that Eu exhibits negative anomaly (Figs. 62 & 63) this is related to the fact that Eu^{2+} is compatible with plagioclase and the removal of plagioclase from the felsic melt by crystal fractionation give rise to negative Eu anomaly. The ratio $(Eu_n)/\sqrt{(Sm_n)(Gd_n)}$ is proposed by Henderson (1984) (Table 1). When the value is >1.0 indicating positive anomaly whilst a value <1.0 points to a negative anomaly. As seen from the table the rocks under consideration are characterized by negative Eu anomaly with varying between 0.47 and 0.61 with an average of 0.54 for the monzogranite. While

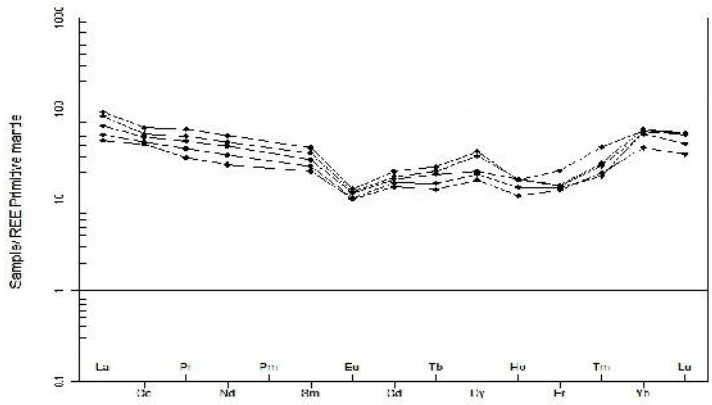

Fig.62: Chondrite-normalized REE's (McDonough & Sun, 1995) of the monzogranite

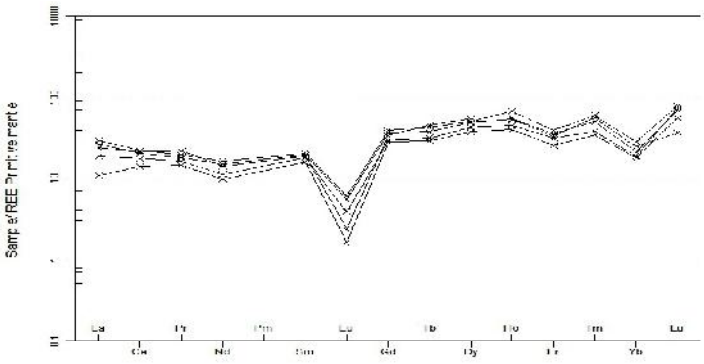

Fig.63: Chondrite-normalized REE's (McDonough & Sun, 1995) of the fluorite-quartz veins.

the analyzed fluorite-quartz veins samples vary from 0.51 to 1.35ppm with an average of 0.76 (Table1).

The analyzed monzogranite shows REEs fractionation where (La/Lu)N vary from 1 to 2.03 with an average of 1.48 and 0.28 to 1.01 with an average of 0.61 for associated fluorite-quartz veins (Table 1). They have relative enrichment of LREE contents in the analyzed monzogranite varying between ∑LREEs 145.04 to 258.1 ppm with an average 197.66. While in the fluorite-quartz veins, the LREEs vary between ∑LREEs 53.25 to 91.31ppm with an average 75.89 (Table 1).

Concerning the HREE, The ∑HREEs vary from 47 to 79.16 ppm with an average 63.95 for monzogranite and ∑HREEs varying between 75.05 and 109.24ppm with an average of 93.46 for associated fluorite-quartz veins. Where the average of (Gd/Lu)n vary from 0.30 to 0.44 with an average of 0.37 for monzogranite and 0.32 to 0.71 with an average of 0.49 for the fluorite-quartz veins samples (Table 1).

Monzogranite shows enrichment of the average of ΣLREEs (197.66) due to presence of allanite and monazite minerals relative to average of ΣHREEs (63.95) (Table 1) due to presence of zircon, xenotime and fluorite. The fluorite-quartz veins show enrichment of the average of ΣHREE's (93.46) relative to average of ΣLREEs (75.89) (Table 1) can be attributed to the influence of fluorite mineral.

The depletion of the total REEs contents in the monzogranite and associated fluorite veins are 261.61 and 169.36 ppm respectively which is less than the average of the world wide granites (270 ppm) as given by Hermann (1970).

The depletion of REEs has been attributed to various processes including magmatic differentiation (Cuney and Friedrich, 1987), hydrothermal leaching (Cathelineau & Holliger, 1987) and or a combination of both. The metasomatic process may also cause severe leaching of REE from the albitized granite. For example the REE depletion may be related to the transformation of accessory minerals such as monazite to apatite and thorite in some albitized granites (Boulvais et al., 2007).

Ce anomaly (Ce/ Ce*= $Ce_n/\sqrt{[La_n * Pr_n]}$) can be useful indicator for the features of fluids, such as temperature, pH and FO_2. The studied monzogranite and fluorite-quartz samples have slightly positive Ce anomalies with average 0.94 and 1.20 respetively (Table 1). Constantopoulos (1988) proposed that, positive Ce anomaly in fluorites depends on high oxygen fugacity in the source of the hydrothermal fluids because of the resultant oxidation of Ce^{3+} and immobilization of Ce^{4+}.

Fluorite samples in the different studied areas reveal positive Y anomalies ($Y/Y^*=Y_n/\sqrt{(Dy_n * Ho_n)}$) with averages 1.64 for monzogranite and 1.08 for fluorite-quartz veins (Table 1). Moller and Holzbercher (1998) proposed that, Y enrichments depend on the presence of fluoride complexes, while Bau and Duliski (1996) mention that, Y-F complexes have high stability when compared with Ho-F complexes. Therefore, Y outshines to stay within fluorite formed from F-rich fluids. Positive Y anomalies articulate strong complexation with F and decoupling of Y from HREE is a common feature in hydrothermal fluids dominated by F complexes (Schönenberger et al, 2008)

RADIOACTIVITY

Both rocks (monzogranite and fluorite-quartz veins) forming G. Adedia are radioactive with different degree, the former is characterized by lower radioactivity relative to the latter. Uranium and thorium contents are measured chemically by fluorometric method in ten samples (5 samples monzogranite and 5 samples fluorite-quartz veins). U ranges from 16 to 32 ppm with an average of 27 ppm while Th ranges from 46 to 72 ppm with an average of in the monzogranite. Fluorite-quartz veins

exhibit higher U values ranging from 79 to 280 ppm with an average of 152.4 ppm and Th from 40 to 83 ppm with an average of 57.8 ppm (Table 1). The highest U and Th and lowest Th/U ratio of fluorite-quartz veins relative to younger granite indicates strong mobilization of uranium from the younger granite.

Plotting U versus Th of the two rocks on the binary diagram shows positive relation between the two elements in monzogranite, this reflect their enrichement with magmatic differentiation (Fig. 64). Fluorite-quartz vein show enrichement of U and Th which might suggest that U and Th had been added post magmatically.

Under magmatic conditions, thorium is generally three times more abundant than uranium i.e. the Th/U ratio is generally around to 3 (chondritic ratio). Th/U ratio in the monzogranite ranges from 1.44 to 3.00 with an average of 2.01, while in the fluorite-quartz veins it ranges from 0.23 to 0.78 with an average of 0.38. The variation between the Th/U ratios and U-contents (Fig. 65) shows negative relation suggests enrichment of uranium relative to thorium which may be attributed to the presence of accessory minerals or that the secondary processes played the main role in uranium enrichment which suggests that uranium was post magmatically added to these granites.

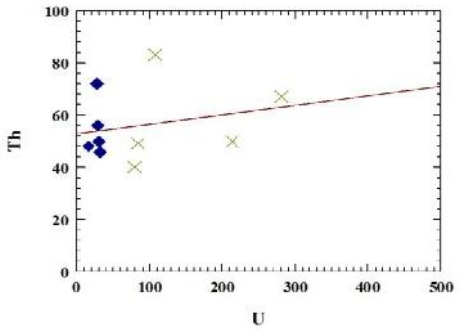

Fig. 64: U-Th ratio of the studied monzogranite rocks and fluorite-quartz veins

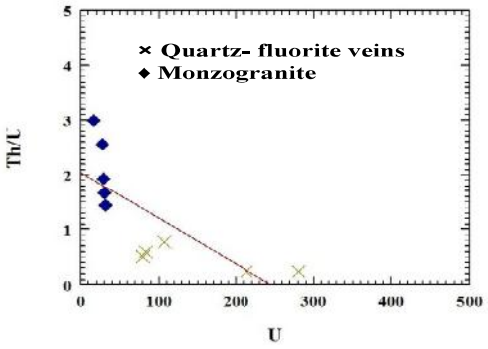

Fig. 65: U-Th/U ratio of the studied monzogranite rocks and fluorite-quartz veins

DISCUSSION

Cathelineau (1987) stated that the uranium mineralization is affected by the different alteration stages, these stages of leaching; mobility and redeposition of U are affected by hydrothermal solutions and supergene fluids.

The sericitization of the granite near the fluorite veins suggested that Ca content is low may be caused by meteoric water leaching and the leached Ca is involved in the formation of fluorite.

Dawood et al., (2010) concluded that the fluoride and carbonate complexes played a significant role in the formation of kasolite. Pre-existing uranium-bearing accessory minerals reacted with high temperature hydrothermal solutions to form urano-fluoride complexes at reducing conditions. When the fluids approached the surface passing through fracture system, the decrease in temperature was associated with the decay of the activity of fluorine ion by the dilution of hydrothermal solutions and precipitation of fluorite. These uranium-carbonate complexes are combined later with silica and lead to form kasolite.

The occurrences of sulphide minerals (pyrite, galena, chalcopyrite, sphalerite, covellite, bornite) induce reducing conditions favorable for the precipitation of radioactive mineralization.

Sminov (1984) suggested that the low Th/U ratio (less than 3) in granitic rocks is due to the effect of fluids carrying uranium mineralization. The studied fluorite-quartz veins have Th/U ratio less than 3 indicating the high effect of hydrothermal solutions.

CONCLUSIONS

The studied monzogranite and associated fluorite-bearing quartz veins represent a part of the basement rocks of Sinai of Egypt. The fluorite-bearing quartz veins are characterized by violet color with greenish color of copper and uranium mineralization.

Geochemical data indicating strong enrichments in some rare metals (Cu,Zn,Zr,Y,Ba,Pb,Nb,U and Th) reaching up to average (57.8, 232, 130.6, 131.2, 74, 127.6 and 23.4 ppm) in monzogranite and (177.8, 234, 114.6, 228.6, 94.4, 240.8 and 20.8 ppm respectively) in fluorite-quartz veins.

The monzogranite is characterized by LREE-enriched pattern with negative Eu anomalies. Relative to the granite, fluorite-quartz veins are depleted in LREE and enriched in HREE and have remarkable negative Eu anomalies. Accessory minerals play an important role in supporting REEs contents in the two rocks; some of them enhance LREEs (allanite, monazite, bastnaesite) in the granites and others enhance HREEs (fluorite, xenotime) in fluorite-bearing quartz veins. These are the most important REE carriers, this explains the differences in REE patterns.

The U contents of the analyzed monzogranite samples range from 16 to 32 ppm with an average of 27 ppm, while the associated fluorite-bearing quartz veins, U contents range from 79 to 280 ppm with an average of 152.4 ppm and Th from 40 to 83 ppm with an average of 57.8 ppm. The studied fluorite veins have low Th/U ratios indicating uranium enrichment due to presence of kasolite mineral.

Acknowledgements

I am indebted to Prof. Amer Bishr of NMA for his field facilities, picking samples and scientific aids of this work. Also many thanks to prof. M. H. Shalaby for the offered help in the revision of the manuscript.

REFERENCES

Ali, H.H., 2016. Uranium and REEs Mineralizations of Wadi El Sahu area, South Western Sinai, Egypt. Ph. D. Thesis, Al-Azhar. Univ., 155p.

Bau, M., and Dulski, P., 1996. Distribution of yttrium and rare-earth elements in the Pengeand Kuruman iron-formations, Transvaal Supergroup, South Africa. Precambrian Res.79,37-55.

Berry, L.G.; Mason, B., and Dietrich, R.V., 1983. Mineralogy. Freeman, San Francisco.

Berry, L.G.; Mason, B, and Dietrich, R.V., 2000. Mineralogy. CBS publishers and distributors, New Delhi, India, 561p.

Bishr, A.H., and Nasr, M.M., 2017. Geological, mineralogical and radioactivity studies of Wadi El-Feraa area Southwestern Sinai, Egypt. Eg. J. Geol., 61.

Bishr, A.H., 2003. Geology, radioactivity, and mineralogical studies of some granitic plutons in Wadi Um Hamd environs, Southwestern Sinai, Egypt. M. Sc. Thesis, Mans. Univ., 132p.

Boulvais, P.; Ruffet, G.; Cornichet, J., and Mermet, M., 2007 Cretaceous albitization and dequartzification of Hercynian peraluminous granite in the Salvezines Massif (French Pyrénées). Lithos, 93, 89–106.

Cathelineau, M., and Holliger, P., 1987. Polyphase metallogenesis of hydrothermal uranium

veins from the southern amoricon massif, France. Proc. Int. Mtg Nancy., 212-217.

Chakhmouradian, A., and Wall, F., 2012. Rare earth elements: minerals, mines, magnets (and more). Elements,8,333-342.

Constantopoulos, J., 1988. Fluid inclusion and REE geochemistry of fluorite from south-central Idaho. Econ. Geol. ,83,626-636.

Cuney, M., and Friedrich, M., 1987. Physicochemical and crystal–chemical controls on accessory mineral paragenesis in granitoids: Implications for uranium metallogenesis. Bull. Mineral.,110, 235-247.

Dawood, Y. H.; Harbi, H.M., and Abdel-Naby, H.H., 2010. Genesis of kasolite associated with aplite-pegmatite at Jabal Sayid, Hijaz region, Kingdom of Saudi Arabia. J. Asian Earth Sci., 37, 1-9.

Deer, W.A.; Howie, R.A., and Zussman, J., 1992. An introduction to the rock forming minerals. Longman Group Limited, London, England. Second edition, 696p.

El Ramly, M.F. and Akaad, M.K., 1960. The basement complex in the central Eastern Desert of Egypt between lat. 24° 30 and 25° 4^N. Geol. Surv. Egypt, paper No. 8, 35P.

El-Gaby, S., 1975. Petrochemistry and geochemistry of some granite from Egypt. N. Jb. Mineral. Abh. 124, 147-189.

Hedrick, J.B., 2004. Rare earths in selected U.S. defense applications: Bloomington, Ind., 40th forum on the Geology of Industrial Minerals. p. 13.

Henderson, P., 1984. Rare earth elements geochemistry. El Sevier Sci. publ., New York. 510p.

Hermann, A.G., 1970 Yttrium and lanthanides. In: Handbook of geochemistry(Wedepohl,Ed.), Springerverlog, New York, U. S. A., 39-57.

Hume, W.F., 1935. Geology of Egypt, Part II. The later plutonic and intrusive rocks. Geol. Surv. Egypt., 301-688.

Karakaya, M.; Karakaya, N.; and Bakir, S., 2011. Some properties and potential applications of the N- and Ca-bentonites of ordu (N.E.Turkey). Appl. Clay Sci., 159-165.

Hussein, A.A., 1990. Mineral deposits. In: The geology of Egypt (Said R.,Ed.). Balkema, Rotterdam, 511-566.

Magotra, R.; Namga S.; Singh, P., and Srivastava, P., 2017. A New Classification Scheme of Fluorite Deposits. Inter. J. Geosciences.8, 599-610.

McDonough, W., and Sun, S., 1995. The composition of the earth. Chem. Geol., 120 (3-4), 223-253.

Möller, P., and Holzbercher, E., 1998. Eu anomalies in hydrothermal fluids and minerals. A combined thermochemical and dynamic phenomenon. Freib Forsch hefte.47573,84. 55.

Pan, Y., and Breaks, F.W., 1997. Rare-earth elements in fluorapatite, Separation Lake area, Ontario: evidence for S-type granite-rare-element pegmatite linkage. Can. Mineral., 35, 659-671.

Read, H.H., 1984. Rutley,s elements of mineralogy. Jain for CBS publishers and Distributors, Delhi, India, 560p.

Reto, G.; Terry, W.; Richard, W., and Katja, R., 2009. Metamict fergusonite-(Y) in a spessartine-bearing granitic pegmatite from Adamello, Italy. Chem. Geol., 261, 333-345.

Roz, M.E., 1994. Geology and uranium mineralization of Gabal Gattar area, North Eastern Desert, Egypt. MSc. Thesis, Fac. Sci., Al Azhar University.

Sabet, A.H.; Tsogoev, V.B.; Spiridonov, V.P.; Sarin, L.P., and Abdel-Nabi, A.A., 1976. Geologic structure and laws of localization of tin-beryllium mineralization at the Igla deposit. Ann Geol Surv

Egypt .6, 157-168.

Sallet, R.; Moritz, R., and Fontignie, D., 2000. Fluorite 87S/86Sr and REE constraints on fluid-melt relations, crystallization time span and bulk DSr of evolved high-silica granite, Tabuleiro granites, Santa Catarina. Brazil Chem Geol . 164,81–92.

Salman, A,B.; El Aassy, I.E., and Shalaby, M.H., 1986. New occurrence of uranium mineralization in Gabal Qattar, Northern Eastern Desert, Egypt. Ann Geol Surv Egypt. 16,31–34.

Schönenberger, J.; Köhler, J., and Markl, G., 2008. REE systematics of fluorides, calcite and siderite in peralkaline plutonic rocks from the Gardar Province, South Greenland. Chem. Geol., 247,16-35.

Shalaby, M.H., 1995. New occurrence of uranium mineralizations GVII, Gabal Qattar uranium prospect, North Eastern Desert. Egypt Bull Fac Sci Alex Univ., 35(2),447–460.

Sminov, S.D., 1984. U-Th-RE mobility in granitic environments at the hydrothermal stage. IAEA, Vienna, 215-246.

Speer, J.A., 1980. Zircon. In Reviews in mineralogy (Ribbe, P. H. ,Ed.), 5, Orthosilicates, 67-112.

معدنية،جيوكيميائية وإشعاعية صخور الجرانيت وعروق الفلوريت-كوارتز المصاحبة، جبل العديدية، منطقة أم بجما، جنوب غرب سيناء، مصر

دعاء انور مصطفى

يهدف هذا البحث إلى دراسة معدنية وجيوكيميائية وإشعاعية صخور الجرانيت وعروق الفلوريت-كوارتز المصاحبه لها الموجودة في الجزء السفلى لمنطقة جبل العديدية ، جنوب غرب سيناء، مصر.

يتميز الجرانيت في جبل العديدية بوجود عروق الكوارتز الغنيه بالفلوريت الحامله لتمعدنات اليورانيوم .

وقد اثبتت الدراسات المعدنيه وجود معادن ثانويه لليورانيوم (الكازوليت) بالاضافه إلى معادن (اليورانوثوريت، الفرجسونيت، المونازيت، الالانيت، الباستنيزيت، الفلوريت، الزركون، الزينوتيم، الاباتيت، البيريت، البارايت، الجالينا، الكالكوبيريت، السفلريت،الكوفليت، البورنيت و الاتكاميت).

إن صخور الجرانيت وعروق الفلوريت المصاحبه لها من الممكن أن تحوي أو تعمل كمصدر لتمعدنات الفلزات النادرة (النحاس والزنك والزركونيوم والإتريوم والباريوم والرصاص والنيوبيوم والثوريوم و اليورانيوم) حيث أن هناك مراحل عديدة من التشوه والتأثر بالمحاليل الحارمائية والصهيرية اثرت على تلك الصخور وكانت مصاحبة لتكون هذه التمعدنات.

توضح نتائج التحاليل الكيميائية للعناصر الارضية النادرة لصخور الجرانيت وعروق الفلوريت المصاحبه لها وجود قيمة سالبة لشاذات الاروبيوم و أن هناك عملية اثراء للعناصر الارضية النادرة الخفيفة مقارنة بالعناصر الأرضية الثقيلة لصخور الجرانيت لاحتوائه معادن

المونازيت، الالانيت والباستنيزيت بينما يوجد عملية اثراء للعناصر الارضية النادرة الثقيلة مقارنة بالعناصر الأرضية الخفيفة لعروق الفلوريت لاحتوائه معادن الفلوريت والزينوتيم .

دراسة تحديد المستوى الاشعاعى اوضحت ان متوسط اليورانيوم والثوريوم لصخور الجرانيت هو 27، 54,4 جزء فى المليون على الترتيب. بينما فى عروق الفلوريت فانه يعادل 152,4، 57,8 جزء فى المليون على الترتيب.